

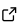


cationCalc4EPMA: Efficient processing tool for EPMA dataset

Kazuki Matsuyama^{1,2}, Yumiko Harigane³, and Yoshihiro Nakamura³

¹ Department of Earth and Planetary Sciences, Graduate School of Environmental Studies, Nagoya University, Japan ² Geosciences Montpellier, Universite de Montpellier, France ³ Research Institute of Geology and Geoinformation, Geological Survey of Japan, National Institute of Advanced Industrial Science and Technology, Japan

DOI: [10.xxxxxx/draft](https://doi.org/10.xxxxxx/draft)

Software

- [Review](#) 
- [Repository](#) 
- [Archive](#) 

Editor: 

Submitted: 13 October 2025

Published: unpublished

License

Authors of papers retain copyright and release the work under a Creative Commons Attribution 4.0 International License ([CC BY 4.0](https://creativecommons.org/licenses/by/4.0/)).

Summary

The cationCalc4EPMA is a freely available MATLAB tool designed to process electron probe microanalysis (EPMA) data by converting oxide weight percentages into cation-based formulas. This conversion is crucial for petrological tasks such as determining structural formulas, estimating $\text{Fe}^{3+}/\text{Fe}^{2+}$ ratios, recognizing solid-solution series, and performing thermobarometric modeling. The tool features automatic mineral identification using empirical composition thresholds and includes built-in functions for calculating commonly used petrological indices, like the Mg\# ($\text{Mg} / (\text{Mg} + \text{Fe})$) for olivine. Additionally, it provides batch averaging based on sample codes to streamline data interpretation. By replacing manual or proprietary workflows, cationCalc4EPMA improves reproducibility, transparency, and accessibility in the geoscientific analysis of EPMA datasets.

Statement of Need

Electron probe microanalysis (EPMA) is a contemporary technique grounded in the physical principles of electron-induced X-ray emission and wavelength-dispersive spectroscopy (WDS), initially developed by Raymond Castaing during his doctoral research in Paris ([Castaing, 1951](#)). This method stands out as one of the most effective microanalytical approaches for conducting precise, non-destructive, and quantitative elemental analysis of solid substances, such as minerals, at the micrometer level ([Yang, 2022](#)). As a result, EPMA is extensively utilized and has profoundly influenced geoscientific studies ([Basch et al., 2024](#); [Kouketsu et al., 2014](#); [Sweatman & Long, 1969](#); [Wiedenbeck et al., 2007](#)). The compositional information derived from EPMA is crucial for interpreting pressure-temperature-time (P - T - t) histories (e.g., [Ozawa, 2004](#)), reconstructing fluid-rock interaction processes (e.g., [Whattam et al., 2022](#)), and assessing geodynamic conditions within the Earth's interior (e.g., [Chardelin et al., 2024](#)).

To extract meaningful petrological insights from EPMA data, it is crucial to convert weight percent values into cation-based formulas, which are typically standardized to a specific number of oxygen atoms or cations, depending on the mineral group. This transformation is essential for calculating structural formulas, evaluating $\text{Fe}^{3+}/\text{Fe}^{2+}$ ratios, identifying solid-solution series, and performing thermobarometric modeling. Ensuring the reproducibility of this conversion method is particularly crucial, as several minerals, including amphibole ([Holland & Blundy, 1994](#); [Putirka, 2016](#); ?), mica (?), and garnet ([Grew et al., 2013](#)), are named based on the calculated cation distribution. Despite its importance, many researchers continue to rely on outdated spreadsheet macros, manual calculations, or proprietary software, all of which are prone to human error and difficult to verify or replicate.

To address this issue, we have created cationCalc4EPMA, a cation calculator for EPMA datasets,

designed for MATLAB. This tool imports .csv files produced by EPMA and transforms weight percent data into cations, adhering to open science principles to enhance reproducibility and transparency. The calculation procedures in cationCalc4EPMA are primarily based on those of Deer et al. (Deer et al., 2013), except for the Fe^{3+} calculation.

To estimate Fe^{3+} , the charge balance method or site allocation method is employed. This approach is tailored for specific minerals: pyroxenes (Papike & Baldwin, 1974), spinel and inverse spinel (Droop, 2018), amphibole (Holland & Blundy, 1994), epidote (Masumoto et al., 2014), and garnet (Enami, 2012). Nonetheless, if verifying the exact amount of Fe^{3+} proves challenging or if its calculated presence might influence the end-member ratio, users have the option to assume $\text{Fe}^{3+} = 0$ by activating the commented-out code.

A key feature of this calculator is its ability to automatically identify the mineral phase from the measured data using empirical mass percentages and subsequently compute the cations. Additionally, the calculator is composed of one module and one .m file, enabling users to easily modify the code to suit their specific requirements, such as for minerals with an extensive list or for calculations tailored to particular data based on location. This design caters to a broader spectrum of users who rely on EPMA analysis.

Methods

cationCalc4EPMA processes EPMA datasets using the following steps:

1. Importing Excel files:

Users choose a raw data file (.csv or .xlsx) from a list dialog. The module Cation_moduli.xlsx, which works alongside the main script, is loaded automatically. This module includes two sheets: one that holds the molar weights, cation numbers, oxygen atom counts, and names of oxides/anions; and another that contains stoichiometric details for target minerals. To add more minerals to the list, users need to update this module accordingly.

2. Creating a mineral list:

Users select the mineral phases anticipated to be present in the raw dataset to create a list of a list of these mineral phases. The potential candidates for this list can be found in the Cation_moduli.xlsx module. This initial list comprises olivine, orthopyroxene (Opx), clinopyroxene (Cpx), spinel, plagioclase, ilmenite, magnetite, quartz, amphibole, chlorite, epidote, biotite, garnet, and apatite, which are typically found in metamorphic and ultramafic rocks. This list plays a crucial role later in the process for automatic mineral identification (Step 9), so it is essential to include the minerals that have been measured.

3. Pre-processing Excel files:

The script is designed to work directly with the EPMA output files. Initial processing steps address any missing data and ready the information for further analysis.

4. Selecting data for cation calculation:

Users have the option to choose which elements to factor into the calculation. The script presumes that the sum of the selected columns (wt%) will be close to 100%. If there are any repeated element names, the process stops, and an error is displayed.

5. Filtering by Detection Limit (DL):

If the file contains DL values, any measurements that fall below the DL are automatically omitted.

6. Renaming dataset variables:

Column (variable) names are renamed to improve readability.

7. Handling missing elements:

87 For elements (e.g., P, V, S) that may not be included in every analysis, NaN-filled dummy
88 columns are added to prevent errors during calculation.

89 8. Creating a total wt% column:

90 The total of the selected wt% columns is calculated for each row.

91 9. Identifying mineral phases:

92 Mineral phases are determined automatically based on empirical composition thresholds.
93 Calculations are then performed for each identified phase. Users must ensure that this
94 classification matches the actual mineral assemblage. Furthermore, since this function is
95 constructed using the if statement, the sequence in which identification is executed is crucial.
96 In the initial script, minerals with distinct compositions are given precedence, followed by the
97 evaluation of silicates. When users introduce new mineral phases, it is advisable for them to
98 determine the “identification” sequence by consulting the commented-out sections within the
99 script.

100 10. Splitting data by mineral phase:

101 The dataset is split into separate tables by assigned mineral names.

102 11. Calculating elemental cation numbers:

103 The cation (or anion) numbers for each element are calculated by dividing the measured data
104 (wt%) by the molar weight.

105 12. Calculating oxygen molar amounts:

106 Oxygen molar quantities are determined using oxide weight percentages and module data. The
107 results are compiled into a single Excel file, organized by mineral.

108 13. Normalizing elemental cation numbers:

109 By utilizing the oxygen molar values and module data, the cation numbers for each element
110 are determined according to the mineral’s theoretical formula. Additionally, petrologically
111 significant indices, such as Mg# for olivine and Almandine% for garnet, are computed.

112 14. Outputting cation calculation results:

113 Results are exported to an Excel file, with separate sheets for each mineral phase.

114 15. Averaging values by sample code:

115 EPMA data often uses sample identifiers like EPMA01_01, EPMA01_02, and so forth, which
116 consist of the rock sample name (sample code) followed by a serial number. The script identifies
117 common prefixes and calculates average values for each mineral associated with each sample
118 code. This approach provides a useful estimate of typical compositions, though users should
119 be aware that zoning or variations in composition within grains could affect interpretation.

120 Package Summary

121 cationCalc4EPMA enables:

122 1. Processing of EPMA data:

123 Facilitates conversion of raw wt% data to cation/anion molar values.

124 2. Automatic mineral identification:

125 Classifies mineral phases based on empirical mass% composition thresholds. These criteria can
126 be modified by the user. The results are output in separate sheets per mineral.

127 3. Calculation of common petrological indices:

128 Calculates commonly used indices, such as Mg# and almandine%, directly from cation data.
 129 4. Sample-based averaging:
 130 Automatically averages values by mineral phase and sample code prefix.

131 Acknowledgement

132 This study was carried out using the electron probe microanalysis (EPMA; JXA-iPF200H) at
 133 GSJ-Lab in AIST, Japan. The authors wish to thank Hiroaki Koge, for recommending this
 134 submission to JOSS. We also thank Tomoaki Morishita, Yui Kouketsu, Katsuyoshi Michibayashi,
 135 and Benoit Ildefonse for their support during this study. This study was supported by grants
 136 from JST SPRING (JPMJSP2125), the Sasakawa Scientific Research Grant from The Japan
 137 Science Society (2024-6011), and the Japan Society for the Promotion of Science, Japan
 138 (JP25KJ1408).

139 License

140 This software is distributed under the MIT License.

141 Basch, V., Godard, M., Tommasi, A., & Rampone, E. (2024). Melt/rock ratios and melt
 142 fluxes during reactive percolation: From matrix- to melt-controlled dynamics [Journal
 143 Article]. *Contributions to Mineralogy and Petrology*, 180(1). <https://doi.org/10.1007/s00410-024-02194-1>
 144

145 Castaing, R. (1951). *Application of electron probes to local chemical and crystallographic*
 146 *analysis* [Thesis].

147 Chardelin, M., Tommasi, A., & Padron-Navarta, J. A. (2024). Progressive strain localiza-
 148 tion and fluid focusing in mantle shear zones during rifting: Petrostructural constraints
 149 from the zabargad peridotites, red sea [Journal Article]. *Journal of Petrology*, 65(8).
 150 [https://doi.org/ARTN egae081 10.1093/petrology/egae081](https://doi.org/ARTN%20egae081%2010.1093/petrology/egae081)

151 Deer, W. A., Howie, R. A., & Zussman, J. (2013). *An introduction to the rock-forming*
 152 *minerals* [Book]. <https://doi.org/10.1180/dhz>

153 Droop, G. T. R. (2018). A general equation for estimating Fe³⁺ concentrations in ferromag-
 154 nesian silicates and oxides from microprobe analyses, using stoichiometric criteria [Journal
 155 Article]. *Mineralogical Magazine*, 51(361), 431–435. <https://doi.org/10.1180/minmag.1987.051.361.10>
 156

157 Enami, M. (2012). Influence of garnet hosts on the raman spectra of quartz inclusions
 158 [Journal Article]. *Journal of Mineralogical and Petrological Sciences*, 107(4), 173–180.
 159 <https://doi.org/10.2465/jmps.111216>

160 Grew, E. S., Locock, A. J., Mills, S. J., Galuskina, I. O., Galuskin, E. V., & Halenius, U.
 161 (2013). Nomenclature of the garnet supergroup [Journal Article]. *American Mineralogist*,
 162 98(4), 785–811. <https://doi.org/10.2138/am.2013.4201>

163 Holland, T., & Blundy, J. (1994). Non-ideal interactions in calcic amphiboles and their bearing
 164 on amphibole-plagioclase thermometry [Journal Article]. *Contributions to Mineralogy and*
 165 *Petrology*, 116(4), 433–447. <https://doi.org/10.1007/bf00310910>

166 Kouketsu, Y., Enami, M., Mouri, T., Okamura, M., & Sakurai, T. (2014). Composite
 167 metamorphic history recorded in garnet porphyroblasts of sambagawa metasediments in
 168 the besshi region, central shikoku, southwest japan [Journal Article]. *Island Arc*, 23(4),
 169 263–280. <https://doi.org/10.1111/iar.12075>

170 Masumoto, Y., Enami, M., Tsuboi, M., & Hong, M. (2014). Magmatic zoisite and epidote in

- 171 tonalite of the ryoke belt, central japan [Journal Article]. *European Journal of Mineralogy*,
172 26(2), 279–291. <https://doi.org/10.1127/0935-1221/2014/0026-2360>
- 173 Ozawa, K. (2004). Thermal history of the horoman peridotite complex: A record of thermal
174 perturbation in the lithospheric mantle [Journal Article]. *Journal of Petrology*, 45(2),
175 253–273. <https://doi.org/10.1093/petrology/egg110>
- 176 Papike, C., J. J., & Baldwin, K. (1974). *Amphiboles and pyroxenes: Characterization of other*
177 *than quadrilateral components and estimates of ferric iron from microprobe data* (Vol. 6,
178 pp. 1053–1054) [Conference Paper].
- 179 Putirka, K. (2016). Amphibole thermometers and barometers for igneous systems and some
180 implications for eruption mechanisms of felsic magmas at arc volcanoes [Journal Article].
181 *American Mineralogist*, 101(4), 841–858. <https://doi.org/10.2138/am-2016-5506>
- 182 Sweatman, T. R., & Long, J. V. P. (1969). Quantitative electron-probe microanalysis of
183 rock-forming minerals [Journal Article]. *Journal of Petrology*, 10(2), 332–379. [https://doi.org/10.1093/](https://doi.org/10.1093/petrology/10.2.332)
184 [petrology/10.2.332](https://doi.org/10.1093/petrology/10.2.332)
- 185 Whattam, S. A., De Hoog, J. C. M., Leybourne, M. I., & Khedr, M. Z. (2022). Link between
186 melt-impregnation and metamorphism of atlantis massif peridotite (IODP expedition
187 357) [Journal Article]. *Contributions to Mineralogy and Petrology*, 177(11). <https://doi.org/10.1007/s00410-022-01968-9>
188 <https://doi.org/10.1007/s00410-022-01968-9>
- 189 Wiedenbeck, M., Hanchar, J. M., Peck, W. H., Sylvester, P., Valley, J., Whitehouse, M.,
190 Kronz, A., Morishita, Y., Nasdala, L., Fiebig, J., Franchi, I., Girard, J. -P., Greenwood,
191 R. C., Hinton, R., Kita, N., Mason, P. R. D., Norman, M., Ogasawara, M., Piccoli, P.
192 M., ... Zheng, Y. -F. (2007). Further characterisation of the 91500 zircon crystal [Journal
193 Article]. *Geostandards and Geoanalytical Research*, 28(1), 9–39. [https://doi.org/10.1111/](https://doi.org/10.1111/j.1751-908X.2004.tb01041.x)
194 [j.1751-908X.2004.tb01041.x](https://doi.org/10.1111/j.1751-908X.2004.tb01041.x)
- 195 Yang, S.-Y. (2022). Electron probe microanalysis in geosciences: Analytical procedures and
196 recent advances [Journal Article]. *Atomic Spectroscopy*, 43(1). [https://doi.org/10.46770/](https://doi.org/10.46770/as.2021.912)
197 [as.2021.912](https://doi.org/10.46770/as.2021.912)